Efficient Bayesian Experiment Design with Equivariant Networks

Conor Igoe* Machine Learning Department Carnegie Mellon University cigoe@cs.cmu.edu

Tejus Gupta* Robotics Institute Carnegie Mellon University tejusg@cs.cmu.edu

Jeff Schneider Robotics Institute Carnegie Mellon University schneide@cs.cmu.edu

Abstract

Recent work in Bayesian Experiment Design (BED) has shown the value of using Deep Learning (DL) to obtain highly efficient adaptive experiment designs. In this paper, we argue that a central bottleneck of DL training for BED is belief explosion. Specifically, as an agent progresses deeper into an experiment, the effective number of realisable beliefs grows enormously, placing significant sampling burdens on offline training schemes in an effort to gather experience from all regions of belief space. We argue that choosing an appropriate inductive bias for actor/critic networks is a critical component in mitigating the effects of belief explosion and has so far been overlooked in the BED literature. We show how Graph Neural Networks are particularly well-suited for BED DL training due to their domain permutation equivariance properties, resulting in multiple orders of magnitude improvement to sample efficiency compared to naive parameterizations.

1 Introduction

Scientific inquiry depends on empirical observations to refine our understanding of the world. These observations generate data that can be analyzed, interpreted, and used to test hypotheses and theories. However, conducting experiments comes with costs, including time, financial resources, and logistical constraints. As a result, determining which observations are most valuable for a given line of inquiry is a central concern in *the Design of Experiments*.

In particular, Bayesian Experiment Design, or BED, has emerged as an elegant formalism for understanding the value of different experiment designs [1, 2]. Moreover, in recent years there has been a growing interest in adopting Deep Learning (DL) and Deep Reinforcement Learning (DRL) techniques to obtain effective experiment designs for BED tasks [3, 4, 5, 6, 7, 8, 9, 10].

Principal among the motivations for the involvement of DL techniques is their potential to increase the scope of problems that admit practical BED solutions [11]. More specifically, practitioners typically trade off decision-theoretic performance with online computational costs when deploying BED policies in real-world tasks. Deep Learning can amortize computationally costly but high-performing BED policies, allowing for improved decision-making, reduced compute burdens, or both. For example, recent work has shown that multistep lookahead-based approaches for achieving non-myopic experiment designs involve considerable online computation in the face of nested integrals. Wu and Frazier [12] describe how these approaches can require up to an hour of compute for a single decision in modest Bayesian Optimization (BO) problems. Although they propose a novel method to reduce this compute overhead to at most several minutes, such online compute requirements are prohibitive in certain high-frequency or resource-constrained tasks, for example in remote

*Equal contribution.

39th Conference on Neural Information Processing Systems (NeurIPS 2025).

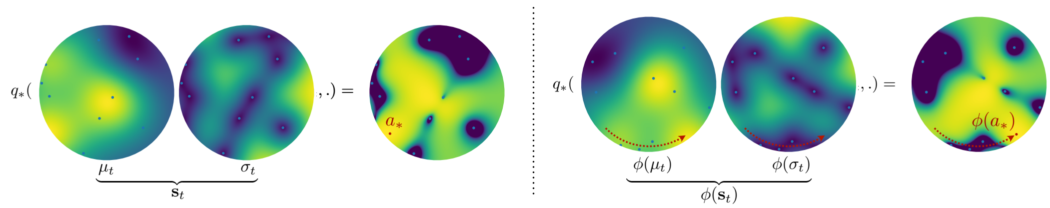

Figure 1: **Illustration of Domain Transformation Equivariance** The figure on the left of the dotted line shows the posterior mean, μ, and marginal standard deviation, σ, of a 2D Gaussian Process, along with the LogEI acquisition function used in Bayesian Optimization. This corresponds to the optimal 1-step lookahead q_* landscape when cast as an MDP, with the optimal action a_* shown in red. The figure on the right shows the same posterior belief state and acquisition function under a transformation ϕ that rotates the domain by 90°. Note that although these belief-action pairs appear different, they are related by the transformation ϕ and represent equivalent decisions under an equivariant policy.

sensing [10] or edge computing [13]. In contrast, amortized policies trained using DRL can achieve non-myopic designs while requiring several orders of magnitude less online computation [4, 10].

Although the recent focus on amortizing expert policies for BED has shown great promise, a core argument of this paper is that existing approaches have significantly high training compute burdens. For example, we find that these approaches can take on the order of days to match the performance of simple experts on modest BED tasks.

We trace this issue to an explosion of possible posterior beliefs as inference progresses through an adaptive experiment, which we call "belief explosion". We observe that existing approaches struggle to learn in the presence of this large diversity of beliefs at deeper timesteps. We argue that designing methods that can cope with this belief explosion efficiently should be a priority for the BED community, and our work proposes to leverage the equivariant structures of optimal BED policies to achieve this goal.

Specifically, we show how a large family of BED tasks admit optimal policies that are *domain permutation equivariant*, and that exploiting this structure leads to significantly more efficient learning in the face of belief explosion. Moreover, as we show in this work, these structural properties naturally suggest an inductive bias that is readily captured in Graph Neural Network (GNN) architectures.

In particular, our contributions are as follows:

- we show that a significant bottleneck when training policies for BED tasks is belief explosion, and show how standard architectures commonly found in the literature are ill-suited to address this challenge;
- we prove that a large family of BED tasks are domain permutation equivariant, which suggests a natural inductive bias for policy and critic networks;
- we demonstrate the utility of leveraging this domain-permutation equivariance on two prominent BED tasks, showing up to two orders of magnitude improvement in sample efficiency compared to various architectures operating on both belief-state and information-set representations;
- we show that GNNs trained on small BED tasks can be used to generalise to significantly larger tasks, resulting in order of magnitude less online compute at test time;
- we show that these equivariances can be extended to information-set-based policies in continuous BED tasks, allowing us to efficiently train performant policies for higher dimensional BO tasks.

2 Notation & Preliminaries

In order to provide a unified notation for our main theoretical and experimental results, we introduce the Bayesian Experiment Design and Markov Decision Process formalisms in the following two subsections, followed by a short overview of Graph Neural Networks.

2.1 Bayesian Experiment Design

Bayesian Experiment Design is a general framework that helps agents make intelligent decisions to efficiently reduce their uncertainty over a set of hypotheses. More specifically, BED models a sequential interaction process, or "experiment", between a decision-making agent and an environment containing some latent variable of interest, denoted θ. A BED task is defined by the tuple $(\Theta, \mathcal{X}, \mathcal{Y}, p_0, p, r)$, where Θ defines a space of possible values for the latent variable, or "hypotheses", $\mathcal{X}$ defines a space of actions available to the agent, or "experiment designs", and $\mathcal{Y}$ defines a space of observations, or "experiment outcomes". The probabilistic models $p_0(\theta)$ and $p(y|x, \theta)$ define a prior over the possible hypotheses and the observation model, respectively.

At each time step $t = 0, 1, \ldots$, the agent chooses the experiment design x_t based on the posterior belief state $p_t := p(\theta|\{(x_\tau, y_\tau)\}_{\tau=0}^{t-1})$. The environment then yields the observation $y_t \sim p(y|x_t, \theta)$, which the agent adds to its information set $\mathcal{I}_t = \{(x_\tau, y_\tau)\}_{\tau=0}^{t-1}$. The agent is interested in choosing informative experiment designs to reduce the uncertainty about θ as measured by some functional of the posterior $r(p(\theta|\mathcal{I}_t))$.

The BED framework is flexible in its ability to model finite hypothesis classes as well as continuous. For example, in this paper we focus on two tasks that feature prominently in the ML and robotics literature as case studies for our experimental results: Bayesian Optimization (BO) and Active Search (AS). BO can be thought of as an instance of a BED task where θ represents some unknown continuous black-box function that must be optimized. Similarly, AS can be thought of as a BED task where θ is a binary-valued vector representing the location of objects of interest in a discredited real-world terrain. We return to more detailed descriptions of the BO and AS tasks in their respective experimental sections.

2.2 Markov Decision Processes

For ease of analysis, we now describe how to view a BED task as an instance of a Markov Decision Process (MDP).

We consider finite-horizon MDPs defined by the tuple $(\mathcal{S}, \mathcal{A}, P, \rho, r, T)$, where the state space $\mathcal{S}$ is continuous and the action space $\mathcal{A}$ is discrete, and the unknown state transition function $P : \mathcal{S} \times \mathcal{S} \times \mathcal{A} \to [0, \infty)$ represents the probability density of the next state $\mathbf{s}_{t+1} \in \mathcal{S}$ given the current state $\mathbf{s}_t \in \mathcal{S}$ and action $\mathbf{a}_t \in \mathcal{A}$. The environment generates a reward $r_t \in \mathbb{R}$ based on the current state $\mathbf{s}_t$ and action $\mathbf{a}_t$. The environment generates trajectories of length $T \in \mathbb{N}$ starting from an initial state drawn from initial state distribution $\rho : \mathcal{S} \to [0, \infty)$. The standard MDP objective is to find a policy $\pi_\varphi : \mathcal{S} \to \mathcal{A}$ by optimizing policy parameters φ to maximize the expected discounted return $\mathbb{E}[\sum_{t=0}^{T-1} r_t|\pi_\varphi]$. Note that we use t to denote the MDP timestep throughout this paper.

For the BED task, we define the MDP state as the posterior belief $\mathbf{s}_t := p_t$, and the action as the design $\mathbf{a}_t := x_t$. The state definition satisfies Markovian dynamics assumptions by stochastically transitioning to state p_{t+1} after incorporating (x_t, y_t) using the inference equations, with stochasticity arising from the random variable y_t. The reward is defined as a functional of p_t, and can involve a variety of application-specific quantities that incorporate information-theoretic terms derived from the posterior belief state, as well as action costs and geometric quantities relating to the geometry of the underlying domain. In the experiment section, we describe some example reward functions that are commonly found in the BED and related literature for our case study environments.

We note that it is also possible to cast BED tasks in the MDP formalism by defining the state $\mathbf{s}_t := \mathcal{I}_t$. The advantage of choosing information set state representations over belief-state representations is that it allows for the training of end-to-end networks that amortize over the inference process mapping from $\mathcal{I}_t$ to p_t, as well as the expected returns and optimal action. This may be attractive in certain contexts, where inference itself is costly. Indeed, this is the approach adopted in [3, 8, 14, 15, 8]. Due to space constraints, in the main paper we present results that leverage discretized belief state representations following previous work [7, 10, 16]. We include additional results on non-discretized information set methods in the Appendix E.2.

2.3 Graph Neural Networks

Graph Neural Networks (GNNs) are a broad family of architectures designed to process data represented as graphs, where entities are modeled as nodes and their interactions as edges. Through iterative message passing, GNNs enable each node to update its representation by aggregating information from its neighbors, thereby capturing relational structure and inductive biases that standard feedforward or convolutional architectures cannot. This makes them especially well-suited to domains where the underlying structure is non-Euclidean or relational.

Over the past several years, GNNs have been successfully applied across a wide range of machine learning and robotics subfields. In representation learning, GNNs underpin molecular property prediction [17], and structure-aware scene understanding [18]. In reinforcement learning and control, GNNs have been used to model multi-agent interactions [19], physical dynamics [20], and robotic manipulation [21], leveraging their ability to encode symmetry and compositional structure. More broadly, GNNs have become a unifying framework for exploiting invariances and equivariances inherent in structured decision-making problems.

In our experiments, we build on these insights by leveraging GNNs to capture important equivariances in Bayesian Experiment Design (BED) tasks. As described in Section 4, our model architecture exploits the graph structure of the belief representation and design space to improve generalization across environments and hypothesis classes.

3 Belief Explosion as a Policy Optimization Bottleneck in BED

In this section, we identify the *belief explosion* issue and identify how it affects policy optimization for BED tasks. More specifically, belief explosion refers to the phenomenon in which the number of possible beliefs an agent must consider becomes intractably large as the search progresses. This is a well-known problem in the POMDP planning literature [22, 23], but has received little attention in the contemporary BED and deep learning communities.

Figure 2 visualizes the belief explosion for a 1D BO task. The figure on the left shows four belief state trajectories, illustrating the increasing diversity of beliefs with time. The figure on the right illustrates this more precisely: As the agent progresses further into the trial, the average divergence between two realizable beliefs increases. This is shown by the blue curve, which measures the KL divergence between canonical representations of the beliefs—the posterior mean vector and covariance matrix—in discretized Gaussian Process prior BO tasks. The orange curve shows that much of this growth is overstated: for each pair of realizable beliefs $(\mathbf{s}, \tilde{\mathbf{s}})$, there exists a transformed belief in the set of all permuted beliefs $\mathcal{B}(\tilde{\mathbf{s}})$ which can have significantly lower divergence with $\mathbf{s}$ compared to its original untransformed representation.

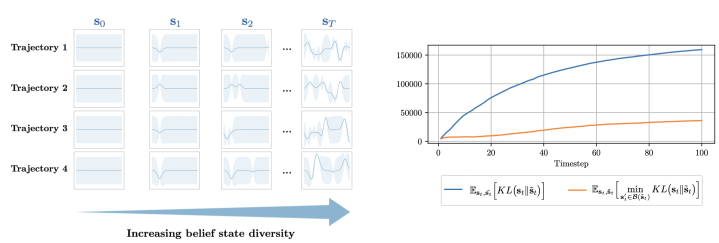

Figure 2: **Belief Explosion**

Next, we show that this rapid increase in $\mathcal{S}_t$ with t renders current policy optimization methods for BED highly sample inefficient when using standard belief representations and network architecture choices. We consider a simple offline learning problem in a small 10-bin discretized 1D BO task. The goal here is to imitate the 1-step greedy expected information gain expert using behavior cloning with a fully connected network trained on $\texttt{concatenate}(\mu_t, \texttt{flatten}(\Sigma_t))$ discretized belief-state representations. Figure 3 shows cross entropy train-test loss curves with an expert data set of 10^4 expert environment transition samples.

Mild overfitting is evident in the left plot of Figure 3 and is perhaps otherwise unremarkable. The figure on the right in Figure 3 shows the same test loss curve but is decomposed over various timesteps. As an example, the green curve shows the test loss when using test beliefs $\{p_3^i\}$ as input to π_φ.

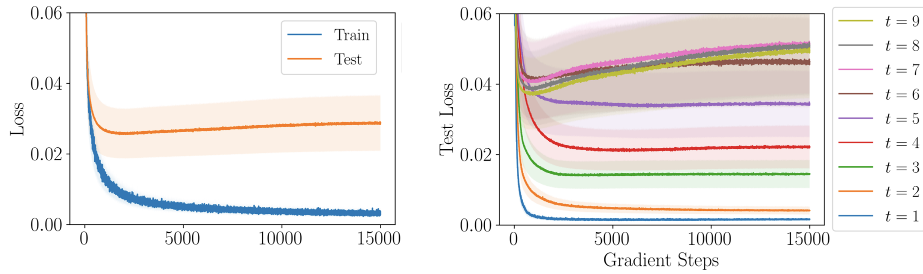

Figure 3: **Test Loss Temporal Decomposition** Note that each curve is averaged over 10 seeds. The shaded region shows ± 2 standard errors.

We make the following observations about Figure 3:

1. The best test loss achieved by π_φ increases monotonically as a function of t until timestep $t = 6$, after which the best test loss stagnates. That is, for "shallow" beliefs, π_φ generalizes well, while for "deep" beliefs, generalization performance plummets. Given that each timestep is associated with the same number of training samples, as is common in standard rollout-based DRL data collection strategies, Figure 3 is a clear illustration of belief explosion in full effect;
2. While the aggregate test curve in left plot of Figure 3 shows mild overfitting, decomposing the test loss over the timesteps tells a very different story: namely, that for shallow beliefs, our network hasn't yet converged to the best test loss, while for deep beliefs, we experience drastic overfitting.

The key issue is that a fully connected network fails to incorporate the structural properties of the BED task, and as a result, it struggles to generalize to unseen belief states at test time. This limitation poses challenges even in very small BO instances, such as this task with only 10 discrete bins.

We argue that embedding BED-specific inductive biases into the model architecture is essential for efficient learning. Our key insight is that naive network parameterizations experience belief explosion along the blue curve of Figure 2, while networks that leverage a property we call *domain permutation equivariance* (introduced in the next section) experience a significantly tamer growth of belief diversity according to the orange curve.

4 Domain-permutation equivariance in BED and GNNs

In this section, we present some intuition about the structural properties of BED tasks that can be exploited for efficient learning. Figure 1 illustrates how we might intuitively expect the acquisition values of belief p_t to be equivariant with respect to a simple transformation of the domain $\mathcal{X}$. We formalize this intuition in our main theoretical result below about the domain-permutation equivariance of optimal policies in BED tasks and use it to motivate the use of GNNs as an appropriate inductive bias.

Specifically, for ease of exposition, we focus our attention on BED tasks in which the posterior belief over the unknown function is fully characterized by the first two moments, as is the case in Bayesian Optimization and Active Search.

Let $f : \mathbb{R}^d \to \mathbb{R}$ be the unknown function which the active sensing agent is querying. We consider BED tasks over a discretised space $\mathcal{X}_{\text{disc}} = \{x^1, x^2, \dots, x^M\}$. The posterior distribution over f (belief-state) given the information set $\mathcal{I}_t$ is therefore a tuple of finite dimensional moments $\mathbf{s}_t = (\mu_t, \Sigma_t)$ with:

$$\mu_t = \big(\mathbb{E}[f(x^i)|\mathcal{I}_t]\big)_{i=1}^M \in \mathbb{R}^M \text{ and } \quad \Sigma_t = \big(\mathbb{E}[\big(f(x^i) - \mu_t^i\big)\big(f(x^j) - \mu_t^j\big)|\mathcal{I}_t]\big)_{i,j=1}^M \in \mathbb{S}_+^M.$$

Consider a set of permutations Φ, where each permutation $\phi \in \Phi$ permutes the belief state $\mathbf{s}_t$. More specifically, each permutation is a bijection $\phi : \{1, 2, \dots, M\} \to \{1, 2, \dots, M\}$ that reorders the indices of the M input points in $\mathcal{X}_{\text{disc}}$. Thus, $\phi(\mathbf{s}_t) = (\mu_{\phi,t}, \Sigma_{\phi,t})$ where:

$$\mu_{\phi,t} = \Big(\mathbb{E}[f(x^{\phi(i)})|\mathcal{I}_t]\Big)_{i=1}^M = \Big(\mu_t^{\phi(i)}\Big)_{i=1}^M,$$

and $$\Sigma_{\phi,t} = \Big(\mathbb{E}\big[\big(f(x^{\phi(i)}) - \mu_t^{\phi(i)}\big) \times \big(f(x^{\phi(j)}) - \mu_t^{\phi(j)}\big)\big|\mathcal{I}_t\big]\Big)_{i,j=1}^{M} = \Big(\Sigma_t^{\phi(i),\phi(j)}\Big)_{i,j=1}^{M}.$$

We overload the notation ϕ to also map actions to permuted actions. In our active sensing setup, each action $\mathbf{a}$ senses some subset of $\mathcal{X}_{\text{disc}}$, i.e., $\mathbf{a} = \mathcal{X}_{\mathbf{a}} \subseteq \mathcal{X}_{\text{disc}}$, and we define $\phi(\mathbf{a}) = \{x^{\phi(i)} : x^i \in \mathcal{X}_{\mathbf{a}}\}$.

Theorem 1 (**Domain Permutation Equivariance).** *Let Φ be a set of permutations. Suppose a Bayesian Experiment Design (BED) task satisfies, for all $\phi \in \Phi$ and all state-action-next-state transitions $\mathbf{s}, \mathbf{s}' \in \mathcal{S}$, $\mathbf{a} \in \mathcal{A}$:*

(i) ***Reward invariance:*** $r(\mathbf{s}, \mathbf{a}) = r(\phi(\mathbf{s}), \phi(\mathbf{a}))$

(ii) ***Transition invariance:*** $p(\mathbf{s}' \mid \mathbf{s}, \mathbf{a}) = p(\phi(\mathbf{s}') \mid \phi(\mathbf{s}), \phi(\mathbf{a}))$

Then, for all $\phi \in \Phi$, all $\mathbf{s} \in \mathcal{S}$, $\mathbf{a} \in \mathcal{A}$, and $\gamma \in [0, 1]$:

$$\pi^*_\gamma(\phi(\mathbf{s})) = \phi(\pi^*_\gamma(\mathbf{s})) \quad \text{(optimal policy equivariance)}$$

$$Q^*_\gamma(\phi(\mathbf{s}), \phi(\mathbf{a})) = Q^*_\gamma(\mathbf{s}, \mathbf{a}) \quad \text{(optimal Q-value invariance).}$$

This reward and transition equivariance property holds for a wide range of BED tasks. For example, with the BO task, a practitioner might choose the reward as the negative posterior argmax entropy. Since the transition is the GP inference, both reward and transition invariance hold, since neither depend explicitly on the ordering of states in the domain. These conditions also hold for the AS task with a more constrained set of permutations, which is described in detail in the appendix.

One way to interpret this result is that using mean *vectors* and covariance *matrices* as belief representations during learning implicitly imposes a fixed ordering on the underlying random variables. This is problematic, as the BED task ultimately requires reasoning about *sets* of jointly distributed random variables, which are inherently unordered. By designing policies that are equivariant to permutations of these variables, we enable agents to generalize optimal behaviors across a broader class of decision-theoretically equivalent belief states, thereby substantially improving sample efficiency.

We emphasize that this theorem is complementary to Theorem 3 by Foster et al. in [3], which concerns *observation-set permutations*. Whereas observation-set permutation invariance focuses on temporal structure, *domain-permutation equivariance* is concerned with the geometric structure of the belief state itself.

The significance of this result is that we can easily generalize between permuted belief states during policy optimization. We use a straightforward way of doing so: using graph representations of the posterior belief as our state, with Graph Neural Networks as our policy class, which are permutation equivariant by design.

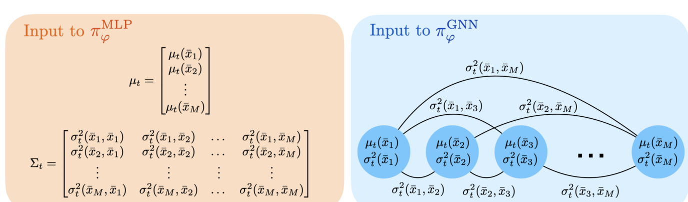

Figure 4: **Dense Network & GNN Comparison: Input Representations** Note that although the graph input to π_φ^{GNN} is a complete graph, we omit all edges from the figure for ease of illustration.

We use a complete undirected graph to represent our belief, with M nodes representing the unknown function value at points in the discretized domain $\mathcal{X}_{\text{disc}}$, and $M(M-1)/2$ edges representing our joint uncertainty between points in $\mathcal{X}_{\text{disc}}$. For example, in the Bayesian Optimisation setting, each node in the graph is labeled with a 2d vector containing posterior statistics $\big(\mu_t(x) = \mathbb{E}(f(x)|\mathcal{I}_t)\,,\, \sigma_t^2(x) = \mathbb{V}(f(x)|\mathcal{I}_t)\big) \in \mathbb{R}^2$. Each edge of the graph is labeled with the posterior covariance $\mathbb{C}\text{ov}\big(f(x)\,,\, f(x') \,|\, \mathcal{I}_t\big) \in \mathbb{R}^+$. We then use a `TransformerConv` architecture [24] for the GNN which transforms labels on the nodes by combining information from the labels in neighboring nodes and edges using learned soft attention. Figure 4 illustrates the input representation to the GNN and the MLP.

5 Experiments

Our experiments aim to answer the following questions:

1. Do GNNs offer an effective inductive bias for efficiently learning BED policies using data from an expensive oracle?
2. Can GNNs be used to learn non-myopic BED policies using reinforcement learning?
3. How well do GNN-based policies transfer across BED problems, and do they scale to larger search problems?

Note that due to space constraints, we leave our reinforcement learning, generalization, and continuous BO experiments in Appendix E.2.

5.1 Setup

Tasks: We use two BED tasks: Bayesian Optimization (BO) and Active Search (AS).

Bayesian Optimization models the problem of efficiently locating the argmax of an unknown function using black-box queries. Our latent variable of interest θ is an unknown function $f : \mathcal{X} \to \mathbb{R}$ defined on the domain $\mathcal{X} \subset \mathbb{R}^d$. The action space $\mathcal{A}$ consists of point locations in the domain $x \in \mathcal{X}$, and the observation model $p(y|x, \theta)$ is a black-box evaluation at the detection location with Gaussian noise $p_{\text{noise}} = \mathcal{N}(0, \sigma^2_{\text{noise}})$. The prior $p(\theta)$ is defined using a zero-mean Gaussian prior with a chosen kernel.

For our experiments, we use a Squared-Exponential kernel $k(x, x') = \sigma^2 \exp\left(-\frac{\|x-x'\|_2^2}{2\ell^2}\right)$. We also discretize the domain $\mathcal{X}$ into a finite set of points $\{x^i\}_{i=1}^M = \mathcal{X}_{\text{disc}} \subset \mathcal{X}$, allowing for exact closed-form inference over the set of random variables $\{f(x^i)\}_{i=1}^M$ using standard Gaussian inference equations [25]. We also restrict the agent's actions to $\mathcal{X}_{\text{disc}}$.

There are several candidate choices for the MDP reward function, but a natural choice [26, 27] for BO tasks is to define $r_t = -\mathcal{H}(p_t^*)$. Here we define p_t^* as the posterior over the $\arg\max$ of f, and we use $\mathcal{H}$ to denote the Shannon entropy. With this reward definition, we incentivize designs that improve the agent's understanding of the location of the maximum of f, or equivalently, designs that reduce the agent's posterior uncertainty about the location of an optimal function value. We note that, unlike posterior inference, there are no closed-form expressions available for $\mathcal{H}(p_t^*)$. We therefore use Monte Carlo sampling to approximate $p_t(x^*)$ with the following estimator:

$$\hat{p}_t(x^*) = \frac{1}{N} \sum_{i=1}^{N} \mathbb{I}\big[\arg\max_x f_i(x) = x^*\big]$$

where $f_i \sim p_t(f)$ and then use $r_t = -\mathcal{H}\big(\hat{p}_t(x^*)\big)$.

We use a 1D domain with $M = 32$ grid points in region length $= 8$ with $\ell = 1$, $\sigma^2_{\text{noise}} = 0.1$ and $\sigma^2 = 1$. These parameters were chosen such that draws $f \sim p_0$ typically have 3-4 local optima, and the smoothness is qualitatively discernible. We set the episode length to $T = 8$. As we shall see, although this toy problem instance may seem trivial, it poses significant challenges when training with standard dense neural networks. In the appendix we explore fully continuous non-discretized BO tasks.

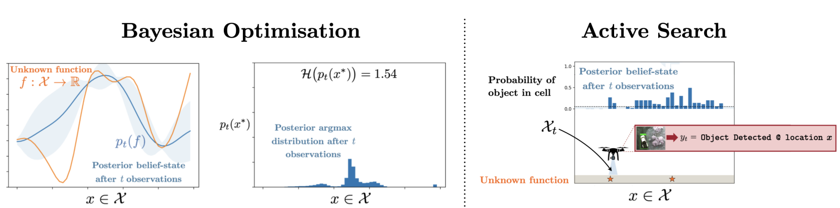

Figure 5: **Overview of the Bayesian Optimization and Active Search Tasks**

Active Search models the problem of efficiently locating sparse objects in an unknown environment by actively taking sensing actions given all observations thus far [28, 29, 30, 31, 32]. Figure 5 illustrates an Active Search problem using an aerial remote sensing agent. We adopt the environment model from [10].

The Active Search problem can be thought of as an instance of the standard Bayesian Optimization problem with some modifications, the key differences being:

1. BO: f smooth; AS: f sparse
2. BO: pointwise sensing of f; AS: contiguous interval sensing of f
3. BO: homoskedastic noise; AS: heteroskedastic noise based on sensed interval $\mathcal{X}_t$.

Here, $f : \mathcal{X} \to \{0, 1\}$ denotes object presence, with $\mathcal{X}$ representing a 1D, 2D, or 3D search space. The prior $p(\theta)$ assumes sparsity. Instead of selecting single points, the agent senses contiguous intervals $\mathcal{X}_t \subseteq \mathcal{X}$, receiving a noisy observation $f(\mathcal{X}_t)$. Wider intervals yield more noise, reflecting the trade-off between resolution and coverage (e.g., higher altitudes capture more area but with less precision).

We adopt the recovery reward, which selects actions to maximize expected detections under the posterior [33, 10, 34].

Experiments use a 1D grid with $M = 32$ and episode length $T = 32$. Actions span up to $l = 4$ points, with noise increasing with interval size—inducing a trade-off between exploration and precision.

Learning-based baselines: We compare GNNs against three standard parameterizations of the policy and critic networks used in previous work: FCNs, CNNs, and Transformers on the information set.

FCN or Dense networks are a naive, but common choice in the DRL literature [35, 36]. Multiple BED DRL papers have used similar architectures while focusing primarily on other dimensions of the BED problem [7, 10].

CNNs, on the other hand, provide a stronger inductive bias for BED tasks [7]. They are set up to predict the Q value or the action probability for each point in the domain using marginal statistics at that point. Although this architecture can be efficient at learning certain functions, it completely ignores the correlations between different points in the domain and, therefore, is insufficient for representing the multistep value function or optimal policy for BED tasks.

Transformers are another promising alternative [37], capable of processing entire information sets directly. Though there is some similarity in transformers and GNNs, they operate on different state representation and offer distinct invariances: transformers directly operate on the information set and provide information set permutation invariance, while the GNNs operate on the belief state and additionally provide domain permutation-set equivariance. Note that in the appendix we include more experiments comparing Transformers and information-set-based GNNs without requiring any discretization strategies.

Non-amortized baselines: For Bayesian Optimization, we compare our learned policies with the greedy policies w.r.t. the Expected Improvement [38] and UCB [39] acquisition functions, as well as Thompson Sampling [40]. For Active Search, we compare with random waypoint selection and a linear sweeping of the search domain [28].

5.2 Behavior Cloning Experiments

We begin our experiments by comparing different policy architectures for behavior cloning an expensive oracle and validating that GNNs offer a helpful inductive bias.

Our goal is to train policies to clone the 1-step greedy expert $\pi_{\text{1-step}} = \arg\max_a \mathbb{E}[r_{t+1}|p_t, a_t = a]$, with a negative posterior argmax entropy reward function. We use Monte Carlo rollouts to generate an offline dataset of beliefs encountered by the 1-step greedy expert, along with the expert actions: $\mathcal{D} = \left\{(p_t^i, a_t^i)\right\}$ where p_t^i denotes the posterior belief state at timestep t in trial i when following policy $\pi_{\text{1-step}}$. In other words, $\mathcal{D}$ is a dataset of (state, actions-of-1-step-expert) collected from the 1-step lookahead policy. The Active Search task uses 32 timesteps per rollout, and the Bayesian

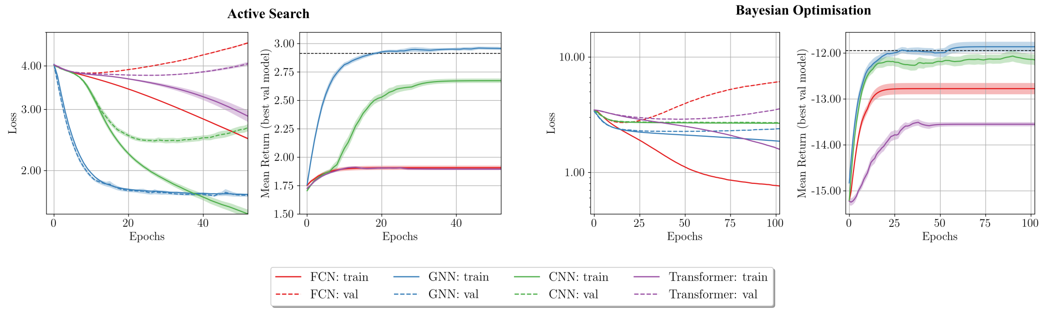

Figure 6: **Comparison of Inductive Biases for Behavior Cloning at 5,000 samples:** Training (solid) and test (dotted) behavior-cloning loss, and expected return for various networks on the Active Search (left) and Bayesian Optimization (right) tasks. The dotted black line denotes the oracle's expected return. During training, we keep track of the best-performing policy on the validation set using the behavior cloning loss (i.e., the rolling best policy). The expected return is then computed by evaluating this best-val policy. Note that each curve is averaged over 5 seeds. The shaded region shows ± 2 standard errors.

Optimisation task uses 8. We note that we include behavior cloning results on BO instances for higher dimensional continuous BO tasks using 32 timesteps in the appendix.

Figure 6 shows the standard train-test loss curves and online performance for different policy networks trained using behavior cloning on AS and BO respectively. We train these networks on an 80:20 train:test split of data from $\mathcal{D}$ using Adam, with varying dataset size $|\mathcal{D}| \in \{50, 500, 5000, 50000\}$ (full results presented in the appendix). The dotted black lines on the right subfigures show the online performance of $\pi_{\text{1-step}}$.

Across both tasks and all dataset sizes, we observe that the GNN shows excellent generalization on the test set, while the other networks overfit and perform poorly on the test set. Moreover, the GNN is able to match the expert's rollout performance using 5,000 samples on both tasks.

Looking at the baselines, we see that the FCN and Transformer are very data-hungry and require a prohibitive number of samples even for small tasks. CNNs improve upon FCNs and Transformers and can learn much more efficiently. However, they are limited by their inability to use cross-correlation terms in the belief state, which is essential for doing well on many BED tasks.

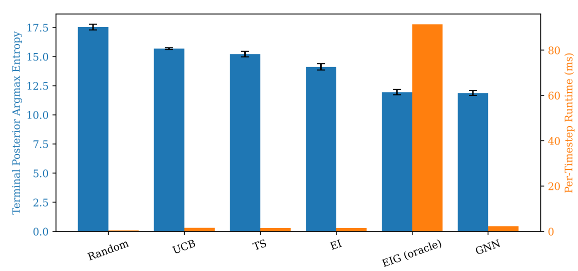

Figure 7: **Comparison with Non-Amortized baselines on BO**

Figure 7 compares the trained GNN with non-learning based baselines: Upper Confidence Bound (UCB), Thompsons Sampling (TS), Expected Improvement (EI) and Expected Information Gain (EIG). We report inference time and performance, as measured by the terminal posterior argmax entropy, that is, the entropy of the posterior argmax implied by the belief state at the final timestep of the rollout ($t = T = 8$). We see that the GNN can match the oracle's performance while being significantly faster. Acquisition functions such as EI and UCB are faster to compute, but don't perform as well.

Our experiments in this section validate our claim that the choice of inductive bias is a bottleneck for efficiently learning BED policies. We show that GNNs are more sample efficient than other networks by at least an order of magnitude on all tasks, confirming the benefit of exploiting the domain-permutation equivariance structure for BED tasks.

5.3 Reinforcement Learning Experiments

In this section we provide results on learning non-myopic policies using reinforcement learning. We use DDQN with nonstationary Q-values, integrated Bellman targets and various critic architectures to learn policies described in Section 2. As with the behavior cloning experiments, we compare the performance of the Graph Neural Networks with the Dense Networks, CNNs, and Transformers.

For the BO enviornment, we use the negative posterior argmax entropy as the reward function. For the AS environment, we use the full recovery rate reward [10].

Figure 8 shows the training curves for our reinforcement learning experiments. The black dotted line shows the performance of the greedy policy. As in the offline training setting, we see significant improvements in training efficiency when using GNNs. In fact, the GNNs are the only policy that can learn non-myopic policies in either task. All other networks train very slowly and we expect them to require at least an order of magnitude more training steps to even reach the myopic policy's performance.

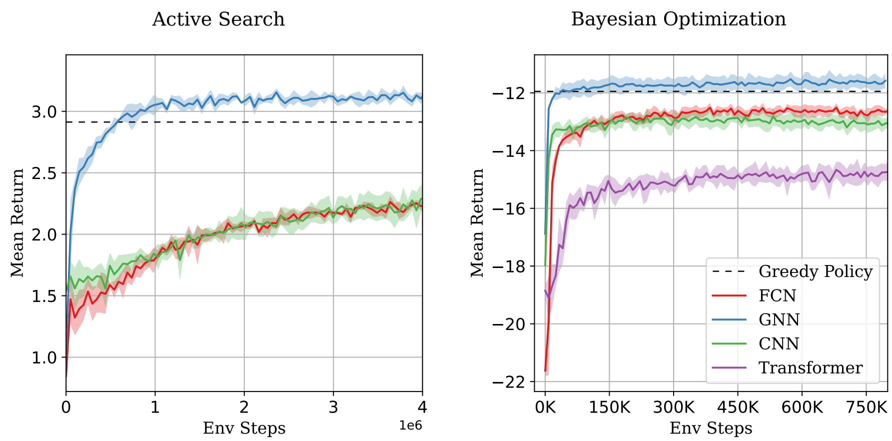

Figure 8: **Comparison of Inductive Biases for Reinforcement Learning:** RL training curves for various architecture on the AS (left) and BO (right) tasks. The dotted black line denotes the oracle's expected return. Note that each curve is averaged over 5 seeds. The shaded region shows ± 2 standard errors.

6 Conclusion

In this work, we identified belief explosion as a bottleneck in policy optimization for BED tasks, and demonstrated that designing networks with the right equivariance structure is an effective strategy at taming this issue. We empirically show that our method can amortize expensive oracles, learn non-myopic policies, and generalize to larger scale BED tasks at test time. We also showed how GNNs can be leveraged in both discrete and continuous contexts, with significantly increased sample efficiency gains in higher-dimensional BO tasks. An exciting future direction involves discovering Φ for a broader range of BED tasks such as SIR parameter identification, as well as expanding our approach to misspecified BED tasks.

Acknowledgments and Disclosure of Funding

This work was supported by the U.S. Army Research Office and the U.S. Army Futures Command under Contract No. W911NF-20-D-0002

We would also like to thank Elissa Wu for her continuous support and encouragement during this project.

References

[1] Dennis V Lindley. On a measure of the information provided by an experiment. *The Annals of Mathematical Statistics*, 27(4):986–1005, 1956.

[2] Kathryn Chaloner and Isabella Verdinelli. Bayesian experimental design: A review. *Statistical Science*, pages 273–304, 1995.

[3] Adam Foster, Desi R Ivanova, Ilyas Malik, and Tom Rainforth. Deep adaptive design: Amortizing sequential bayesian experimental design. In *International Conference on Machine Learning*, pages 3384–3395. PMLR, 2021.

[4] Adam Foster, Martin Jankowiak, Elias Bingham, Paul Horsfall, Yee Whye Teh, Thomas Rainforth, and Noah Goodman. Variational bayesian optimal experimental design. *Advances in Neural Information Processing Systems*, 32, 2019.

[5] Adam Foster, Martin Jankowiak, Matthew O'Meara, Yee Whye Teh, and Tom Rainforth. A unified stochastic gradient approach to designing bayesian-optimal experiments. In *International Conference on Artificial Intelligence and Statistics*, pages 2959–2969. PMLR, 2020.

[6] Takashi Goda, Tomohiko Hironaka, Wataru Kitade, and Adam Foster. Unbiased mlmc stochastic gradient-based optimization of bayesian experimental designs. *SIAM Journal on Scientific Computing*, 44(1):A286–A311, 2022.

[7] Michael Volpp, Lukas P Fröhlich, Kirsten Fischer, Andreas Doerr, Stefan Falkner, Frank Hutter, and Christian Daniel. Meta-learning acquisition functions for transfer learning in bayesian optimization. *arXiv preprint arXiv:1904.02642*, 2019.

[8] Samuel Müller, Noah Hollmann, Sebastian Pineda Arango, Josif Grabocka, and Frank Hutter. Transformers can do bayesian-inference by meta-learning on prior-data. In *Fifth Workshop on Meta-Learning at the Conference on Neural Information Processing Systems*, 2021.

[9] Vincent Lim, Ellen Novoseller, Jeffrey Ichnowski, Huang Huang, and Ken Goldberg. Policy-based bayesian experimental design for non-differentiable implicit models. *arXiv preprint arXiv:2203.04272*, 2022.

[10] Conor Igoe, Ramina Ghods, and Jeff Schneider. Multi-agent active search: A reinforcement learning approach. *IEEE Robotics and Automation Letters*, 7(2):754–761, 2022.

[11] Tom Rainforth, Adam Foster, Desi R Ivanova, and Freddie Bickford Smith. Modern bayesian experimental design. *Statistical Science*, 39(1):100–114, 2024.

[12] Jian Wu and Peter Frazier. Practical two-step lookahead bayesian optimization. *Advances in neural information processing systems*, 32, 2019.

[13] Mahadev Satyanarayanan. The emergence of edge computing. *Computer*, 50(1):30–39, 2017.

[14] Tom Blau, Edwin V Bonilla, Iadine Chades, and Amir Dezfouli. Optimizing sequential experimental design with deep reinforcement learning. In *International conference on machine learning*, pages 2107–2128. PMLR, 2022.

[15] Samuel Müller, Matthias Feurer, Noah Hollmann, and Frank Hutter. Pfns4bo: In-context learning for bayesian optimization. In *International Conference on Machine Learning*, pages 25444–25470. PMLR, 2023.

[16] Anindya Sarkar, Nathan Jacobs, and Yevgeniy Vorobeychik. A partially-supervised reinforcement learning framework for visual active search. *Advances in Neural Information Processing Systems*, 36:12245–12270, 2023.

[17] Justin Gilmer, Samuel S Schoenholz, Patrick F Riley, Oriol Vinyals, and George E Dahl. Neural message passing for quantum chemistry. In *International conference on machine learning*, pages 1263–1272. Pmlr, 2017.

[18] Peter W Battaglia, Jessica B Hamrick, Victor Bapst, Alvaro Sanchez-Gonzalez, Vinicius Zambaldi, Mateusz Malinowski, Andrea Tacchetti, David Raposo, Adam Santoro, Ryan Faulkner, et al. Relational inductive biases, deep learning, and graph networks. *arXiv preprint arXiv:1806.01261*, 2018.

[19] Philip Kwaku Adjei, Qin Zhiguang, Isaac Amankona Obiri, Ansu Badjie, Christian Nii Aflah Cobblah, Ali Alqahtani, Yeong Hyeon Gu, and Mugahed A Al-Antari. A graph attention network-based multi-agent reinforcement learning framework for robust detection of smart contract vulnerabilities. *Scientific Reports*, 15(1):29810, 2025.

[20] Alvaro Sanchez-Gonzalez, Nicolas Heess, Jost Tobias Springenberg, Josh Merel, Martin Riedmiller, Raia Hadsell, and Peter Battaglia. Graph networks as learnable physics engines for inference and control. In *International conference on machine learning*, pages 4470–4479. PMLR, 2018.

[21] Yixin Lin, Austin S Wang, Eric Undersander, and Akshara Rai. Efficient and interpretable robot manipulation with graph neural networks. *IEEE Robotics and Automation Letters*, 7(2):2740–2747, 2022.

[22] Adhiraj Somani, Nan Ye, David Hsu, and Wee Sun Lee. Despot: Online pomdp planning with regularization. *Advances in neural information processing systems*, 26, 2013.

[23] Yuanfu Luo, Haoyu Bai, David Hsu, and Wee Sun Lee. Importance sampling for online planning under uncertainty. *The International Journal of Robotics Research*, 38(2-3):162–181, 2019.

[24] Yunsheng Shi, Zhengjie Huang, Shikun Feng, Hui Zhong, Wenjin Wang, and Yu Sun. Masked label prediction: Unified message passing model for semi-supervised classification. *arXiv preprint arXiv:2009.03509*, 2020.

[25] Carl Edward Rasmussen. *Gaussian processes in machine learning*. Springer, 2004.

[26] Daniel Hernández-Lobato, Jose Hernandez-Lobato, Amar Shah, and Ryan Adams. Predictive entropy search for multi-objective bayesian optimization. In *International conference on machine learning*, pages 1492–1501. PMLR, 2016.

[27] Zi Wang and Stefanie Jegelka. Max-value entropy search for efficient bayesian optimization. In *International Conference on Machine Learning*, pages 3627–3635. PMLR, 2017.

[28] Nikhil Angad Bakshi, Tejus Gupta, Ramina Ghods, and Jeff Schneider. Guts: Generalized uncertainty-aware thompson sampling for multi-agent active search. In *2023 IEEE International Conference on Robotics and Automation (ICRA)*, pages 7735–7741. IEEE, 2023.

[29] Arundhati Banerjee, Ramina Ghods, and Jeff Schneider. Multi-agent active search using detection and location uncertainty. In *2023 IEEE International Conference on Robotics and Automation (ICRA)*, pages 7720–7727. IEEE, 2023.

[30] Roman Garnett, Yamuna Krishnamurthy, Donghan Wang, Jeff Schneider, and Richard Mann. Bayesian optimal active search on graphs. In *Ninth Workshop on Mining and Learning with Graphs*. Citeseer, 2011.

[31] Roman Garnett, Yamuna Krishnamurthy, Xuehan Xiong, Jeff Schneider, and Richard Mann. Bayesian optimal active search and surveying. *arXiv preprint arXiv:1206.6406*, 2012.

[32] Robin R Murphy. Human-robot interaction in rescue robotics. *IEEE Transactions on Systems, Man, and Cybernetics, Part C (Applications and Reviews)*, 34(2):138–153, 2004.

[33] Ramina Ghods, Arundhati Banerjee, and Jeff Schneider. Decentralized multi-agent active search for sparse signals. In Cassio de Campos and Marloes H. Maathuis, editors, *Proceedings of the Thirty-Seventh Conference on Uncertainty in Artificial Intelligence*, volume 161 of *Proceedings of Machine Learning Research*, pages 696–706. PMLR, 27–30 Jul 2021.

[34] Nikhil Angad Bakshi, Tejus Gupta, Ramina Ghods, and Jeff Schneider. Guts: Generalized uncertainty-aware thompson sampling for multi-agent active search. In *2023 IEEE International Conference on Robotics and Automation (ICRA)*, pages 7735–7741, 2023.

[35] Marcin Andrychowicz, Anton Raichuk, Piotr Stańczyk, Manu Orsini, Sertan Girgin, Raphael Marinier, Léonard Hussenot, Matthieu Geist, Olivier Pietquin, Marcin Michalski, et al. What matters in on-policy reinforcement learning? a large-scale empirical study. *arXiv preprint arXiv:2006.05990*, 2020.

[36] Conor Igoe, Swapnil Pande, Siddarth Venkatraman, and Jeff Schneider. Multi-alpha soft actor-critic: Overcoming stochastic biases in maximum entropy reinforcement learning. In *2023 IEEE International Conference on Robotics and Automation (ICRA)*, pages 7162–7168. IEEE, 2023.

[37] Lei Song, Chenxiao Gao, Ke Xue, Chenyang Wu, Dong Li, Jianye Hao, Zongzhang Zhang, and Chao Qian. Reinforced in-context black-box optimization. *arXiv preprint arXiv:2402.17423*, 2024.

[38] Donald R Jones, Matthias Schonlau, and William J Welch. Efficient global optimization of expensive black-box functions. *Journal of Global optimization*, 13:455–492, 1998.

[39] Niranjan Srinivas, Andreas Krause, Sham M Kakade, and Matthias Seeger. Gaussian process optimization in the bandit setting: No regret and experimental design. *arXiv preprint arXiv:0912.3995*, 2009.

[40] Daniel Russo and Benjamin Van Roy. Learning to optimize via posterior sampling. *Mathematics of Operations Research*, 39(4):1221–1243, 2014.

[41] Maximilian Balandat, Brian Karrer, Daniel R. Jiang, Samuel Daulton, Benjamin Letham, Andrew Gordon Wilson, and Eytan Bakshy. BoTorch: A Framework for Efficient Monte-Carlo Bayesian Optimization. In *Advances in Neural Information Processing Systems 33*, 2020.

[42] Sebastian Ament, Samuel Daulton, David Eriksson, Maximilian Balandat, and Eytan Bakshy. Unexpected improvements to expected improvement for bayesian optimization. *Advances in Neural Information Processing Systems*, 36:20577–20612, 2023.

[43] José Miguel Hernández-Lobato, Matthew W Hoffman, and Zoubin Ghahramani. Predictive entropy search for efficient global optimization of black-box functions. *Advances in neural information processing systems*, 27, 2014.

A Limitations

This work has several limitations. First, all experiments are conducted on synthetic Bayesian experiment design task instances. While these are widely used benchmarks, they do not capture the full complexity of real-world applications. Second, we assume well-specified models throughout, which may not hold in practice. Finally, our framework presumes access to exact posterior moments (e.g., means and covariances), which is appropriate under fixed priors. However, many practical BED settings involve hyperpriors (such as distributions over kernel lengthscales) that induce posterior distributions over parameters for which first- and second-order moments may no longer be sufficient. This complicates the construction of GNN input representations and poses a challenge for generalizing our approach.

B Compute Resources

All experiments in this paper were conducted on a cluster of 8 NVIDIA 2080 Ti GPUs. The longest-running experiments involved training the 10 Transformer model seeds on the 8D Bayesian Optimization continuous behavior cloning task, which took approximately one week.

C Proof of Theorem 1

Theorem 1 (Domain Permutation Equivariance). *If our BED task has the following two properties for all permutations $\phi \in \Phi$:*

1. $r(s,a) = r(\phi(s), \phi(a))$ *(reward invariance)*
2. $p(s'|s,a) = p(\phi(s')|\phi(s), \phi(a))$ *(transition invariance)*

then, for all permutations $\phi \in \Phi$ for all beliefs s for all discounts γ, $\pi^*_\gamma(\phi(s)) = \phi(\pi^*_\gamma(s))$ (optimal policy equivariance)

Proof: We'd like to prove that $\pi^*_\gamma(s) = \phi^{-1}(\pi^*_\gamma(\phi(s)))\ \forall s$. This is equivalent to showing that

$$\arg\max_a q^*(s,a) = \phi^{-1}(\arg\max_a q^*(\phi(s), a))\ \forall s \tag{1}$$

We will also show that

$$q^*(s,a) = q^*(\phi(s), \phi(a)))\ \forall s, \forall a \tag{2}$$

We will prove both Eq 1 and Eq 2 using induction.

Let's start with the last timestep T. Eq 2 directly holds from reward equivariance.
Proof for Eq 1 at the last timestep:

$\phi^{-1}(\arg\max_a q^*_T(\phi(s), a)) = \phi^{-1}(\arg\max_a r(\phi(s), a))$
(the action-value function at timestep T is equal to the reward)

$\implies \phi^{-1}(\arg\max_a q^*_T(\phi(s), a)) = \arg\max_a r(\phi(s), \phi(a))$
(using $\arg\max_x f(\phi(x)) = \phi^{-1}(\arg\max_x f(x))\ \forall f, \phi$)

$\implies \phi^{-1}(\arg\max_a q^*_T(\phi(s), a)) = \arg\max_a r(s,a)$
(using reward invariance)

$\implies \phi^{-1}(\arg\max_a q^*_T(\phi(s), a)) = \arg\max_a q^*_T(s,a)$.

Now we'd like to show that if Eq 1 and Eq 2 holds for timestep $t+1$, it is also true for timestep t.

$$\phi^{-1}(\arg\max_a q_t^*(\phi(s), a)) = \phi^{-1}(\arg\max_a r(\phi(s), a) + \gamma\mathbb{E}_{s'|\phi(s),a}[\max_{a'} q_{t+1}^*(s', a')])$$

(Bellman equation)

$$\implies \phi^{-1}(\arg\max_a q_t^*(\phi(s), a)) = \arg\max_a r(\phi(s), \phi(a)) + \gamma\mathbb{E}_{s'|\phi(s),\phi(a)}[\max_{a'} q_{t+1}^*(s', a')]$$

(using $\arg\max_x f(\phi(x)) = \phi^{-1}(\arg\max_x f(x))$)

$$\implies \phi^{-1}(\arg\max_a q_t^*(\phi(s), a)) = \arg\max_a r(s, a) + \gamma\mathbb{E}_{s'|\phi(s),\phi(a)}[\max_{a'} q_{t+1}^*(s', a')]$$

(reward invariance)

$$\implies \phi^{-1}(\arg\max_a q_t^*(\phi(s), a)) = \arg\max_a r(s, a) + \gamma\mathbb{E}_{s'|s,a}[\max_{a'} q_{t+1}^*(\phi(s'), a')]$$

(transition invariance)

$$\implies \phi^{-1}(\arg\max_a q_t^*(\phi(s), a)) = \arg\max_a r(s, a) + \gamma\mathbb{E}_{\phi(s')|\phi(s),\phi(a)}[\max_{a'} q_{t+1}^*(\phi^{-1}(s'), \phi(a'))]$$

(change of variables: $\mathbb{E}_{\phi(x)}[f(x)] = \mathbb{E}_x[f(\phi^{-1}(x))]$)

$$\implies \phi^{-1}(\arg\max_a q_t^*(\phi(s), a)) = \arg\max_a r(s, a) + \gamma\mathbb{E}_{s'|s,a}[\max_{a'} q_{t+1}^*(\phi^{-1}(s'), a')]$$

(transition invariance)

$$\implies \phi^{-1}(\arg\max_a q_t^*(\phi(s), a)) = \arg\max_a r(s, a) + \gamma\mathbb{E}_{s'|s,a}[\max_{a'} q_{t+1}^*(\phi^{-1}(s'), \phi^{-1}(a'))]$$

(invariance of $\max$ under ϕ)

$$\implies \phi^{-1}(\arg\max_a q_t^*(\phi(s), a)) = \arg\max_a r(s, a) + \gamma\mathbb{E}_{s'|s,a}[\max_{a'} q_{t+1}^*(s', a')]$$

(inductive assumption: Eq. 2 holds for $t + 1$)

$$\implies \phi^{-1}(\arg\max_a q_t^*(\phi(s), a)) = \arg\max_a q_t^*(s, a) = q^*(s, a)$$

This completes our proof by induction. □

D Discrete Belief Representations and Policy Inputs

E Further Experiments

E.1 Full Behavior Cloning Experements

In this section, we present the full results from our behavior cloning experiments described in section 5.2

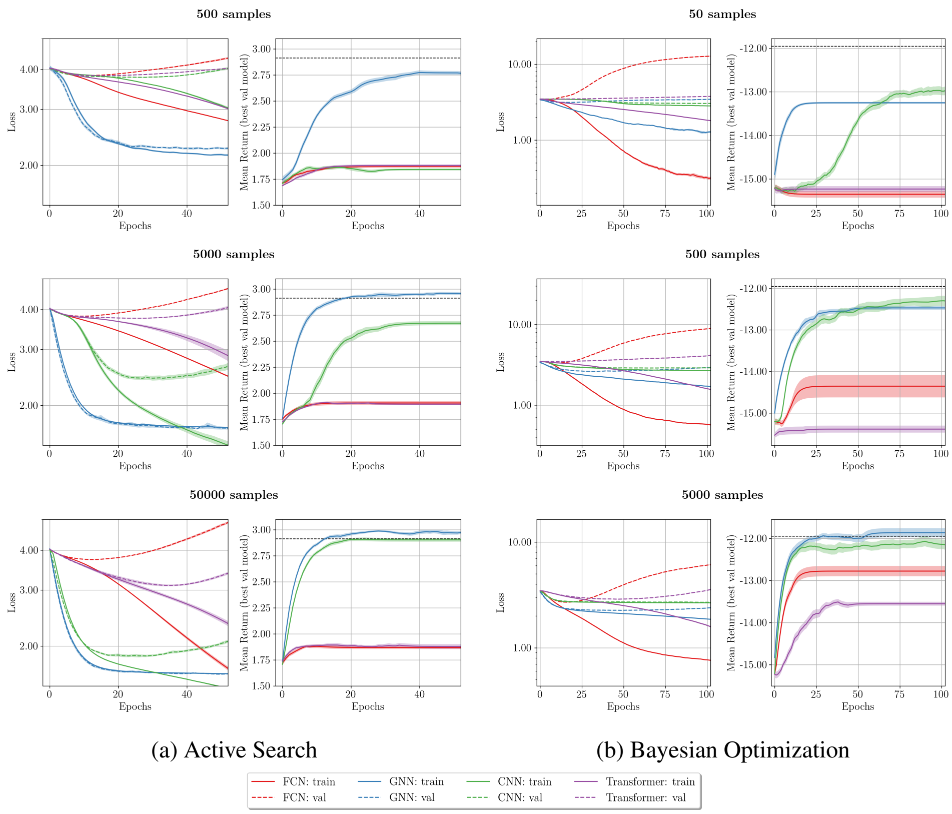

(a) Active Search (b) Bayesian Optimization

Figure 9: **Comparison of Inductive Biases for Behavior Cloning:** We plot the (i) train (solid lines) and test (dotted lines) behavior-cloning loss and (ii) expected return for various networks on the Active Search (left) and Bayesian Optimization (right) tasks using increasing dataset size (top to bottom). The dotted black line denotes the oracle's expected return. Note that each curve is averaged over 5 seeds. The shaded region shows the 95% confidence interval for the mean.

E.2 Generalization and Scaling Experiments

In this section, we evaluate whether GNN-based policies can scale to large search domains where established acquisition functions are prohibitively expensive to compute. We show results on three transfer setups in Table 2-4, training the GNN policy on a smaller problem and evaluating transfer performance on larger versions of the problem in each setup.

For example, Table 1, 2 show the performance of a GNN trained using behavior cloning a greedy expert on a 8×8 active search environment, and evaluated on a 32×32 environment. The GNN almost matches the performance of the expert on the 8×8 grid, and allows us to scale to 32×32 grid. In contrast, it's computationally intractable to run the greedy search on the larger grid because it requires us to estimate the expected information gain for each candidate action, which in turn involves nested integrals. Table 4 and 5 similarly show that GNN-based policies can scale to higher-dimensional tasks and larger grids, and match or outperform expert performance.

Table 1: **Active Search Scaling (Train: 8×8 grid)**

Method	Performance	Time (ms)
Random	15.28 ± 0.32	< 0.01
Simple Search	12.67 ± 0.27	< 0.01
Greedy Search	$\mathbf{35.72 \pm 0.40}$	265.4
GNN	34.13 ± 0.49	3.34

Table 2: **Active Search Scaling (Test: 32×32 grid)**

Method	Performance	Time (ms)
Random	3.72 ± 0.08	< 0.01
Simple Search	3.16 ± 0.07	< 0.01
Greedy Search	N.A.	$> 1e4$
GNN	$\mathbf{7.15 \pm 0.12}$	67.50

F Continuous BO Experiments

Here we present results of experiments comparing the simple regret performance of Transformer and GNN models trained to clone the behavior of the LogEI policy acting on various continuous BO tasks (2D, 4D, 8D), each rollout using $T = 32$ timesteps. In these experiments, no discretization is used: both the Transformer and GNN take the information set $\mathcal{I}_t$ as input and output a point directly in continuous design space, $\mathbf{a}_t \in \mathcal{X} \subseteq \mathbb{R}^d$. This is desirable for contexts where discretization is inappropriate for the level of precision demanded by the application or where it is necessary to additionally amortize inference as well as acquisition estimation and optimization.

We use the BoTorch [41] implementation of LogEI as our expert oracle with default hyperparameters as recommended in their documentation [2]. This oracle is a numerically robust implementation of the canonical Expected Improvement acquisition function, as described in [42]. We use a zero mean Gaussian noise assumption with noise variance of 10^{-6}.

We train both the Transformer and the GNN models on expert trajectories using standard behaviour cloning losses. Table 3 shows the key architectural details of both models.

Table 3: Transformer and GNN hyperparameters for continuous BO experiments

Model	**Trainable Params**	**Hidden Dim**	**# Heads**	**# Layers**
Transformer	$\sim 1 \times 10^7$	40	8	10
GNN	$\sim 1 \times 10^7$	64	8	10

As in the discrete case, the GNN input is a graph constructed from the information set $\mathcal{I}_t$. Specifically, we use the same basic architecture as in the discrete experiments, but here our graph contains $t-1$ nodes at timestep t instead of a fixed number of nodes for all timesteps to match a desired level of discretization. The nodal features are the observed values $\{y_\tau\}_{\tau=0}^{t-1}$, and the edge feature for edge i, j is the kernel evaluation $k(x_i, x_j)$. In the discrete experiments, the GNN output logits for the discrete set of actions. This allowed the network to naturally take advantage of domain transformation equivariance. In these continuous experiments, we transform the nodal features to a final set

[2] https://botorch.org/

of linear weights $\{w_\tau\}_{\tau=0}^{t-1}$ which are used to combine the points in the information set to define an action distribution for the next timestep:

$$\mathbf{a}_t \sim \mathcal{N}\Big(\sum_{\tau=0}^{t-1} w_\tau x_\tau \, , \, \sigma^2 \Big) \text{ where } \{w_\tau\} = f_\theta^{\text{GNN}}(\mathcal{I}_t).$$

This parameterization is equivariant to the same set of transformations Φ that the kernel k is invariant to. Note that in the discrete context, $\Phi \ni \phi : [N] \to [N]$ is a permutation of the discretized domain, while in this continuous setting we abuse notation and use $\Phi \ni \phi : \mathbb{R}^d \to \mathbb{R}^d$ to denote pointwise invertible transformations of the domain. In our experimental results below, we again use an RBF kernel with a lengthscale of 0.2, 0.3, 0.4, for $d = 2, 4, 8$, over an optimization domain refined to the disk $\mathcal{X} = \left\{ x \in \mathbb{R}^d \;\middle|\; \|x\|_2 \leq 0.5 \right\}$. This results in $\Phi = \mathrm{O}(d)$, where $\mathrm{O}(d)$ denotes the orthogonal group, the group of distance-preserving transformations of d-dimensional Euclidean space. We use a fixed variance actor while training both the GNN and Transformer, and during simple-regret rollouts we act deterministically by following the mean policy $\mathbf{a}_t = \sum_{\tau=0}^{t-1} w_\tau x_\tau$. Finally, note that we warm-start the information sets in every rollout with $d + 1$ uniformly at random chosen points in $\mathcal{X}$ for all methods. Timestep 0 in the figure below refers to the first meaningful decision after the warm-start points have already been collected.

The figures below show that GNNs significantly outperform Transformers when trained with the same dataset, with increased delta as BO task dimension increases. The GNN can come close to the simple regret performance of the expert in each task with at least an order of magnitude less data than the Transformer. Moreover, both GNN and Transformer save roughly 1 order of magnitude test-time compute by amortizing the inference, acquisition evaluation and optimization necessary for the BoTorch LogEI expert.

These results demonstrate that our primary equivariance insight is not just restricted to discrete domains. This is important, since real-world BED tasks often involve continuous modeling choices to enable precise experiment designs.

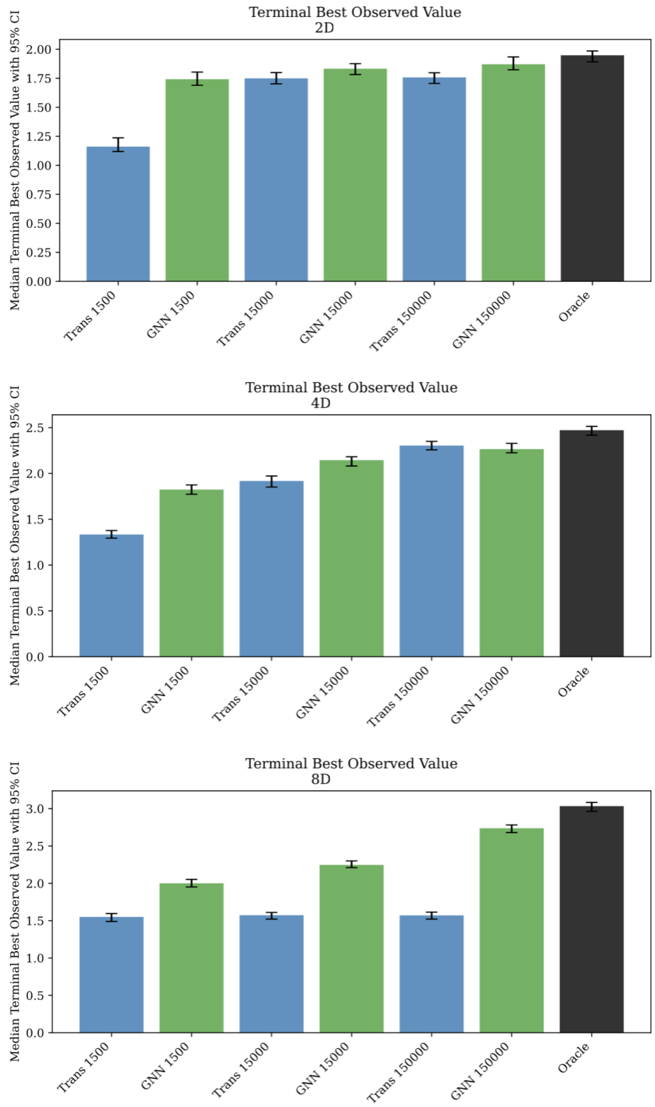

Figure 10: **Continuous BO experimental results.** We use 1,000 rollouts to evaluate the terminal best observed value. Note that optimizing this quantity is equivalent to optimizing simple regret. Here we use median and 1,000-seed bootstrap confidence intervals as is standard in continuous BO literature due to the heavy-tailed nature of simple regret curves in continuous BO, such as in [43]. Both the GNN and Transformer models were trained until overfitting on the indicated number of expert rollout trajectories, with 200 trajectories held out for validation. The simple performance is then computed using the models that achieved the lowest behavior cloning validation loss.

G Additional Generalisation Results

In this section, we evaluate the generalization capabilities of our amortized BO policies across search domain dimensions and sizes. Note that these results use discrete belief representations as in the main paper.

Table 4 reports results for a policy trained on a 2D BO task and then evaluated on a set of higher-dimensional BO tasks. We use an adaptively discretized domain inspired by Volpp et al. [7] (explained below) to keep the size of the belief state tractable. The GNN was trained by behavior cloning the Expected Improvement (EI) policy using 5,000 samples, and was evaluated zero-shot on the 3D and 5D tasks. We compare its performance with a random policy, Thompson Sampling

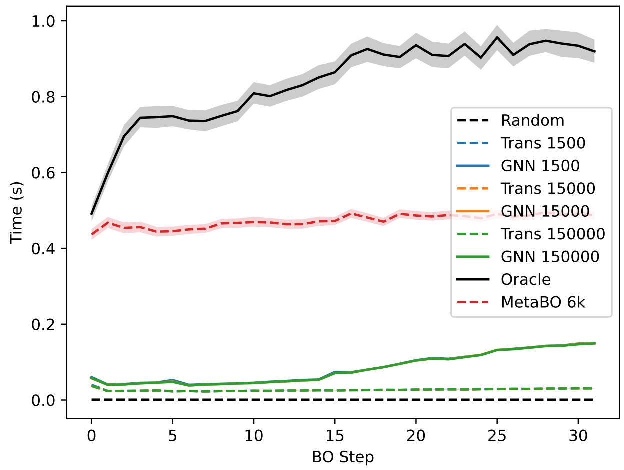

Figure 11: **Continuous BO timing results.** We additionally include a MetaBO variant of the LogEI expert that restricts the acqusition function optimisation to the adaptive discretisatino grid proposed in MetaBO paper [7]. Note that amortized methods significantly outperform non-amortized methods on wall clock time while maintaining comparable performance in terms of simple regret.

(TS), and the EI policy restricted to the discrete domain points. We note that the GNN matches the EI policy's performance on the 2D training task and generalizes well to the 3D and 5D domains.

Table 5 presents another generalization experiment: we train the GNN by behavior cloning the Expected Information Gain (EIG) policy on a domain of $[0, 4]$ discretized into 32 bins using 5,000 samples, and tested on a larger domain of $[0, 128]$ discretized into 1,024 bins. Once again, the GNN shows strong imitation and zero-shot generalization. Note that, due to the computational cost of the EIG policy (exceeding 10 seconds per decision), direct evaluation on the large domain is infeasible. This underscores the value of generalizable amortized policies.

Table 4: **Scaling Amortized BO Policies with Search Dimension**

	Train: 2D		Test: 3D		Test: 5D	
Method	Performance	Time (ms)	Performance	Time (ms)	Performance	Time (ms)
Random	1.07 ± 0.05	0.02	1.13 ± 0.05	0.02	1.13 ± 0.05	0.02
TS	1.25 ± 0.05	1.13	1.29 ± 0.05	1.86	1.23 ± 0.05	1.04
EI	$\mathbf{1.31 \pm 0.05}$	0.29	$\mathbf{1.48 \pm 0.06}$	0.30	$\mathbf{1.48 \pm 0.05}$	1.94
GNN	$\mathbf{1.28 \pm 0.05}$	67.01	$\mathbf{1.49 \pm 0.06}$	56.32	$\mathbf{1.47 \pm 0.05}$	57.46

Table 5: **Scaling Amortized BO Policies with Grid Size**

	Train: $N = 32$		Test: $N = 1024$	
Method	Performance	Time (ms)	Performance	Time (ms)
Random	-15.43 ± 0.17	0.05	-33.79 ± 0.27	< 0.11
TS	-13.44 ± 0.20	0.21	-29.21 ± 0.38	29.11
UCB	-13.74 ± 0.17	0.15	-29.10 ± 0.33	0.24
EIG	$\mathbf{-11.95 \pm 0.20}$	1067.4	N.A.	$> 1e4$
GNN	$\mathbf{-11.60 \pm 0.20}$	9.83	$\mathbf{-27.94 \pm 0.36}$	70.63

Adaptive discretization method: Sample n points uniformly at random in the domain, choose the top k using the EI acquisition function, and then sample m points near each of these k best points. The candidate set consists of $n + km$ points. We use $n = 100, k = 5, m = 20$.

Evaluation procedure: For all the experiments in this section, we evaluate the mean return of the policy using a fixed episode length of 8, averaged over 200 trials, using the EI reward for Table 4 and EIG reward for Table 5. Since the EI reward requires a previous max-value, instead of assuming a fixed initial max value, we choose to initialize each trial with a single point chosen uniformly at random in the domain. This point does not contribute to the timestep count in our experiments.

H Generalization through data augmentation

In this experiment, we compare two different strategies for leveraging the domain permutation equivariant structure in Bayesian Optimization policies for efficient behavior-cloning: (i) using a network with a suitable inductive bias, i.e., the Graph Neural Network described in Section 4, and (ii) applying data augmentation during training. This data augmentation corresponds to the set of permutations the policy is equivariant to.

Figure 12 shows the behavior-cloning training and validation loss alongside the resulting policy performance across several network architectures. Additionally, it shows outcomes from training a fully connected network (FCN) using data augmentation. The results indicate that data augmentation significantly improves the generalization capability of the FCN, as evidenced by the near-perfect alignment of training and validation loss curves (depicted in purple). However, this improvement comes at a substantial computational cost—training times are considerably prolonged. Notably, the GNN achieves expert-level performance within approximately 30 epochs, whereas the FCN augmented with permutation-based data augmentation fails to match this performance even after 7,000 epochs. This disparity is expected since the equivariant permutation set is very large, equal to $n!$ for a n-bin discrete BO task. This is the number of permutation the GNN is naturally equivariant to, but the FCN needs explicit data augmentation for during training. For this particular experiment, the number of permutations is $n! = 32! \approx 2.6 \times 10^{35}$.

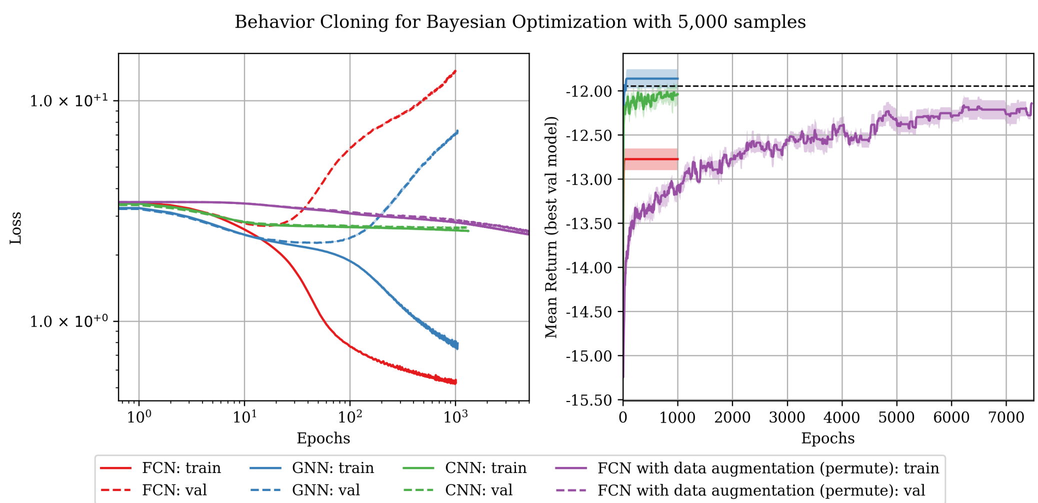

Figure 12: **Comparison of Inductive Biases and Data Augmentation for Behavior Cloning:** We plot the (i) train (solid lines) and test (dotted lines) behavior-cloning loss and (ii) expected return for various networks on the Bayesian Optimization using a dataset size of 5,000 samples. The oracle's expected return is indicated by the dotted black line. Regular training was terminated at 1,000 epochs after performance had stagnated. Note that each curve is averaged over 5 seeds. The shaded region shows the 95% confidence interval for the mean.

I Generalization and Scalability for Bayesian Optimization

In this section, we discuss the generalizability and scalability of our amortized approach to Bayesian Optimization (BO).

I.1 Generalizability

In all but the scaling experiments of section H, our experimental setup assumes a well-specified prior: both training and test functions are sampled from a known Gaussian Process (GP) prior.

While this assumption facilitates controlled evaluation, it does not always hold in practice. Real-world applications of BO often involve misspecified priors, where the true function does not match the assumed GP prior. In these cases, surrogate models are fit by estimating GP hyperparameters from data.

To generalize our amortization approach beyond the well-specified regime, the learned policy should (i) train on a distribution of BED tasks induced by our prior distribution over hyperparameters, and (ii) condition on the posterior distribution over the full set of random variables in the BED task, which now includes the hyperparameters.

I.2 Scalability

Our approach can help with scalability by amortizing the computationally expensive BO methods via a neural policy that maps belief states to actions, thereby reducing online computational burden. However, special care is required in representing the belief state. Our method relies on an explicit representation of the posterior over the search space, which can become prohibitively expensive in high-dimensional settings. In particular, a naïve uniform discretization leads to a grid whose size grows exponentially with the number of input dimensions.

To mitigate this, we adopted a simple adaptive discretization strategy inspired by MetaBO [7] for our higher dimensional BO experiments in section G. By concentrating representational capacity in high-mean or high-uncertainty regions, we retain a tractable belief representation. Nonetheless, the choice of discretization remains a critical factor, and a more principled exploration of this design choice is left to future work.

J Network Hyperparamters for Discrete Experiments

Table 6: **Hyperparameters for FCN.**

Hidden Layers	[512, 512, 512]

Table 7: **Hyperparameters for CNN.**

Number of Layers	6
Kernel size	9

Table 8: **Hyperparameters for GNN.**

Hidden Dim	64
Number of Heads	8
Number of Layers	2

Table 9: **Hyperparameters for Transformer.**

Number of Layers	5
Number of Heads	16
Embedding Size	64

K Training Hyperparamters

Table 10: **Behavior Cloning Hyperparameters**

Learning Rate	3e-4
Batch Size	32
Optimizer	Adam

Table 11: **Reinforcement Learning Hyperparameters**

Algorithm	DDQN
Exploration	ϵ-greedy
Discount factor	0.95
Learning Rate	3e-4
Batch Size	32
Optimizer	Adam

We also use non-stationary Q-functions with DDQN since we model our BED tasks as finite-horizon MDPs. In addition, we use integrated Bellman targets to reduce noise in training.

L Visualisation of Evolution of GNN & FCN Critic

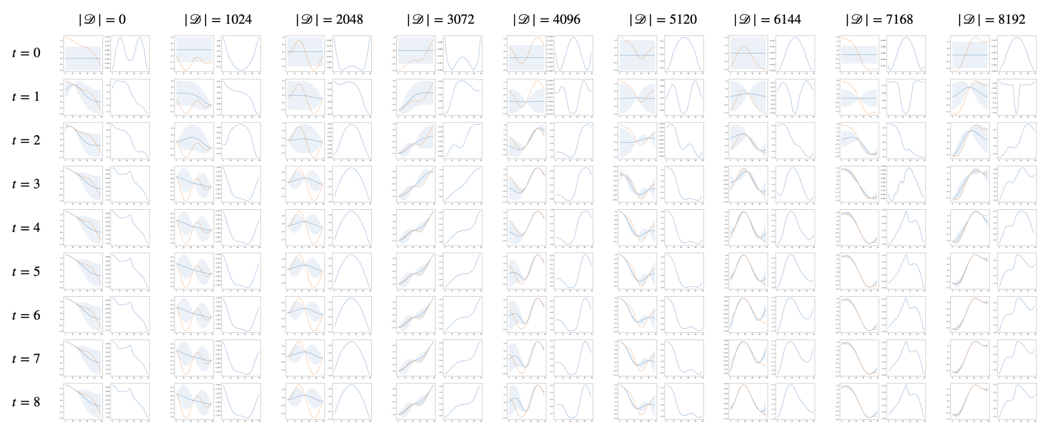

Figure 13: **Evolution of BO GNN policy through RL training.** Each column illustrates a rollout after a given number of collected MDP transitions (indicated in the column title). The left figure in each column depicts the belief state p_t and ground-truth hidden function, and the right figure illustrates the estimated q-values. Note that the GNN quickly learns myopic search behavior (first check both corners of the domain). After gathering more experience, it instead learns to first query the internal point of the domain to act less greedy while maximizing return. Note also that the GNN from initialisation captures symmetry and smoothness priors, and that after 8,192 transitions has learned to represent both sharp discontinuities and smoothness, which is essential when modeling the drop in value for re-sensing a previously queried point, but sharp increase in value for querying neighboring points if the observed point is high.

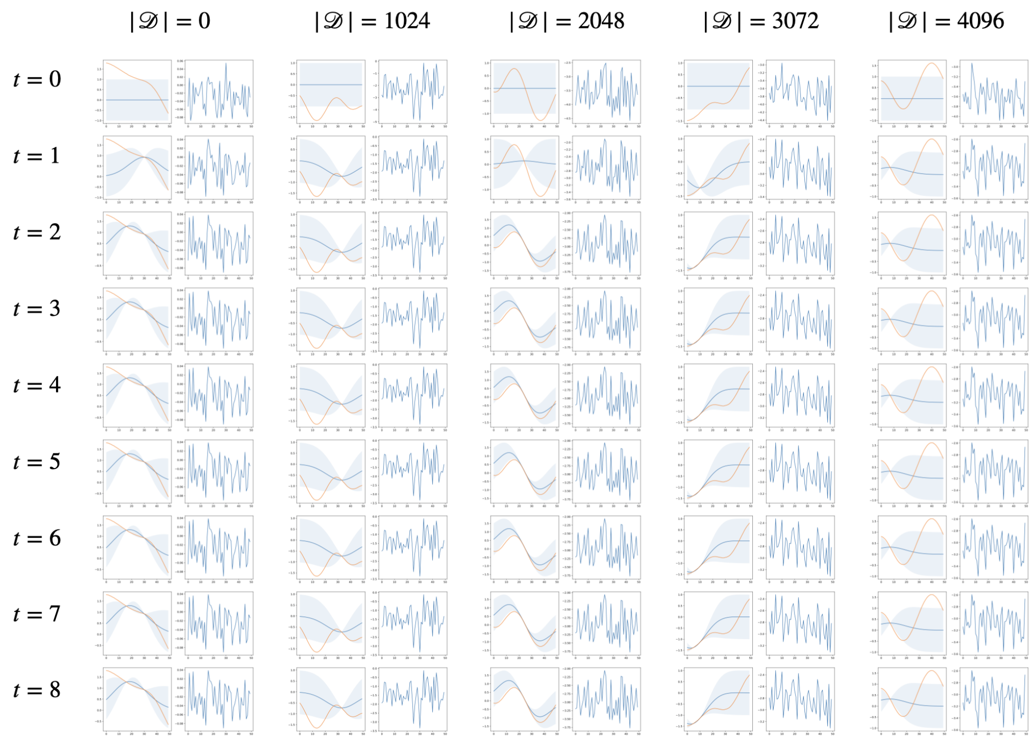

Figure 14: **Evolution of BO FCN policy through RL training.** Each column illustrates a rollout after a given number of collected MDP transitions. The left figure in each column depicts the belief state p_t, and the right figure illustrates the estimated q-values. Note that no qualitative improvement to the q-values is visible after 4,096 MDP transitions, in contrast to the GNN which achieves high rewards and clear structure in the q-estimates.

NeurIPS Paper Checklist

1. **Claims**

   Question: Do the main claims made in the abstract and introduction accurately reflect the paper's contributions and scope?

   Answer: [Yes]

   Justification: The main claims in the abstract and introduction concern the belief explosion problem as a bottleneck for sample efficient BED DL training, the role of domain permutation equivariance as an exploitable property of BED tasks, and the role of GNNs as an inductive bias to leverage this.

   Guidelines:

   - The answer NA means that the abstract and introduction do not include the claims made in the paper.
   - The abstract and/or introduction should clearly state the claims made, including the contributions made in the paper and important assumptions and limitations. A No or NA answer to this question will not be perceived well by the reviewers.
   - The claims made should match theoretical and experimental results, and reflect how much the results can be expected to generalize to other settings.
   - It is fine to include aspirational goals as motivation as long as it is clear that these goals are not attained by the paper.

2. **Limitations**

   Question: Does the paper discuss the limitations of the work performed by the authors?

   Answer: [Yes]

Justification: We have included a limitations section in the appendix of the paper.

Guidelines:

- The answer NA means that the paper has no limitation while the answer No means that the paper has limitations, but those are not discussed in the paper.
- The authors are encouraged to create a separate "Limitations" section in their paper.
- The paper should point out any strong assumptions and how robust the results are to violations of these assumptions (e.g., independence assumptions, noiseless settings, model well-specification, asymptotic approximations only holding locally). The authors should reflect on how these assumptions might be violated in practice and what the implications would be.
- The authors should reflect on the scope of the claims made, e.g., if the approach was only tested on a few datasets or with a few runs. In general, empirical results often depend on implicit assumptions, which should be articulated.
- The authors should reflect on the factors that influence the performance of the approach. For example, a facial recognition algorithm may perform poorly when image resolution is low or images are taken in low lighting. Or a speech-to-text system might not be used reliably to provide closed captions for online lectures because it fails to handle technical jargon.
- The authors should discuss the computational efficiency of the proposed algorithms and how they scale with dataset size.
- If applicable, the authors should discuss possible limitations of their approach to address problems of privacy and fairness.
- While the authors might fear that complete honesty about limitations might be used by reviewers as grounds for rejection, a worse outcome might be that reviewers discover limitations that aren't acknowledged in the paper. The authors should use their best judgment and recognize that individual actions in favor of transparency play an important role in developing norms that preserve the integrity of the community. Reviewers will be specifically instructed to not penalize honesty concerning limitations.

3. **Theory assumptions and proofs**

   Question: For each theoretical result, does the paper provide the full set of assumptions and a complete (and correct) proof?

   Answer: [Yes]

   Justification: We include a full proof in the appendix for our theorem concerning optimal policy equivariance.

   Guidelines:

   - The answer NA means that the paper does not include theoretical results.
   - All the theorems, formulas, and proofs in the paper should be numbered and cross-referenced.
   - All assumptions should be clearly stated or referenced in the statement of any theorems.
   - The proofs can either appear in the main paper or the supplemental material, but if they appear in the supplemental material, the authors are encouraged to provide a short proof sketch to provide intuition.
   - Inversely, any informal proof provided in the core of the paper should be complemented by formal proofs provided in appendix or supplemental material.
   - Theorems and Lemmas that the proof relies upon should be properly referenced.

4. **Experimental result reproducibility**

   Question: Does the paper fully disclose all the information needed to reproduce the main experimental results of the paper to the extent that it affects the main claims and/or conclusions of the paper (regardless of whether the code and data are provided or not)?

   Answer: [Yes]

   Justification: algorithmic and BED environment hyperparameter details, as well as model references are provided in the paper and appendix.

Guidelines:

- The answer NA means that the paper does not include experiments.
- If the paper includes experiments, a No answer to this question will not be perceived well by the reviewers: Making the paper reproducible is important, regardless of whether the code and data are provided or not.
- If the contribution is a dataset and/or model, the authors should describe the steps taken to make their results reproducible or verifiable.
- Depending on the contribution, reproducibility can be accomplished in various ways. For example, if the contribution is a novel architecture, describing the architecture fully might suffice, or if the contribution is a specific model and empirical evaluation, it may be necessary to either make it possible for others to replicate the model with the same dataset, or provide access to the model. In general. releasing code and data is often one good way to accomplish this, but reproducibility can also be provided via detailed instructions for how to replicate the results, access to a hosted model (e.g., in the case of a large language model), releasing of a model checkpoint, or other means that are appropriate to the research performed.
- While NeurIPS does not require releasing code, the conference does require all submissions to provide some reasonable avenue for reproducibility, which may depend on the nature of the contribution. For example
  (a) If the contribution is primarily a new algorithm, the paper should make it clear how to reproduce that algorithm.
  (b) If the contribution is primarily a new model architecture, the paper should describe the architecture clearly and fully.
  (c) If the contribution is a new model (e.g., a large language model), then there should either be a way to access this model for reproducing the results or a way to reproduce the model (e.g., with an open-source dataset or instructions for how to construct the dataset).
  (d) We recognize that reproducibility may be tricky in some cases, in which case authors are welcome to describe the particular way they provide for reproducibility. In the case of closed-source models, it may be that access to the model is limited in some way (e.g., to registered users), but it should be possible for other researchers to have some path to reproducing or verifying the results.

5. **Open access to data and code**

   Question: Does the paper provide open access to the data and code, with sufficient instructions to faithfully reproduce the main experimental results, as described in supplemental material?

   Answer: [No]

   Justification: We have not provided a full codebase for this paper. However, our contribution is in articulating a specific problem independent of specific code implementation, and our results rely on open source widely used GNN, Transformer, CNN and FCN models.

   Guidelines:

   - The answer NA means that paper does not include experiments requiring code.
   - Please see the NeurIPS code and data submission guidelines (`https://nips.cc/public/guides/CodeSubmissionPolicy`) for more details.
   - While we encourage the release of code and data, we understand that this might not be possible, so "No" is an acceptable answer. Papers cannot be rejected simply for not including code, unless this is central to the contribution (e.g., for a new open-source benchmark).
   - The instructions should contain the exact command and environment needed to run to reproduce the results. See the NeurIPS code and data submission guidelines (`https://nips.cc/public/guides/CodeSubmissionPolicy`) for more details.
   - The authors should provide instructions on data access and preparation, including how to access the raw data, preprocessed data, intermediate data, and generated data, etc.
   - The authors should provide scripts to reproduce all experimental results for the new proposed method and baselines. If only a subset of experiments are reproducible, they should state which ones are omitted from the script and why.

- At submission time, to preserve anonymity, the authors should release anonymized versions (if applicable).
- Providing as much information as possible in supplemental material (appended to the paper) is recommended, but including URLs to data and code is permitted.

6. **Experimental setting/details**

   Question: Does the paper specify all the training and test details (e.g., data splits, hyper-parameters, how they were chosen, type of optimizer, etc.) necessary to understand the results?

   Answer: [Yes]

   Justification: We have provided these details in the appendix.

   Guidelines:

   - The answer NA means that the paper does not include experiments.
   - The experimental setting should be presented in the core of the paper to a level of detail that is necessary to appreciate the results and make sense of them.
   - The full details can be provided either with the code, in appendix, or as supplemental material.

7. **Experiment statistical significance**

   Question: Does the paper report error bars suitably and correctly defined or other appropriate information about the statistical significance of the experiments?

   Answer: [Yes]

   Justification: We report standard errors in all figures and describe our approach in detail.

   Guidelines:

   - The answer NA means that the paper does not include experiments.
   - The authors should answer "Yes" if the results are accompanied by error bars, confidence intervals, or statistical significance tests, at least for the experiments that support the main claims of the paper.
   - The factors of variability that the error bars are capturing should be clearly stated (for example, train/test split, initialization, random drawing of some parameter, or overall run with given experimental conditions).
   - The method for calculating the error bars should be explained (closed form formula, call to a library function, bootstrap, etc.)
   - The assumptions made should be given (e.g., Normally distributed errors).
   - It should be clear whether the error bar is the standard deviation or the standard error of the mean.
   - It is OK to report 1-sigma error bars, but one should state it. The authors should preferably report a 2-sigma error bar than state that they have a 96% CI, if the hypothesis of Normality of errors is not verified.
   - For asymmetric distributions, the authors should be careful not to show in tables or figures symmetric error bars that would yield results that are out of range (e.g. negative error rates).
   - If error bars are reported in tables or plots, The authors should explain in the text how they were calculated and reference the corresponding figures or tables in the text.

8. **Experiments compute resources**

   Question: For each experiment, does the paper provide sufficient information on the computer resources (type of compute workers, memory, time of execution) needed to reproduce the experiments?

   Answer: [Yes]

   Justification: We have described the compute resources used in all of our experiments in the appendix.

   Guidelines:

   - The answer NA means that the paper does not include experiments.

- The paper should indicate the type of compute workers CPU or GPU, internal cluster, or cloud provider, including relevant memory and storage.
- The paper should provide the amount of compute required for each of the individual experimental runs as well as estimate the total compute.
- The paper should disclose whether the full research project required more compute than the experiments reported in the paper (e.g., preliminary or failed experiments that didn't make it into the paper).

9. **Code of ethics**

   Question: Does the research conducted in the paper conform, in every respect, with the NeurIPS Code of Ethics `https://neurips.cc/public/EthicsGuidelines`?

   Answer: [Yes]

   Justification: We have reviewed the NeurIPS Code of Ethics and believe that we conform in every respect.

   Guidelines:

   - The answer NA means that the authors have not reviewed the NeurIPS Code of Ethics.
   - If the authors answer No, they should explain the special circumstances that require a deviation from the Code of Ethics.
   - The authors should make sure to preserve anonymity (e.g., if there is a special consideration due to laws or regulations in their jurisdiction).

10. **Broader impacts**

    Question: Does the paper discuss both potential positive societal impacts and negative societal impacts of the work performed?

    Answer: [NA]

    Justification: Our paper studies a specific bottleneck in a purely synthetic context that is of broad interest to the BED community but which we believe is not directly related to any clear broader social impact.

    Guidelines:

    - The answer NA means that there is no societal impact of the work performed.
    - If the authors answer NA or No, they should explain why their work has no societal impact or why the paper does not address societal impact.
    - Examples of negative societal impacts include potential malicious or unintended uses (e.g., disinformation, generating fake profiles, surveillance), fairness considerations (e.g., deployment of technologies that could make decisions that unfairly impact specific groups), privacy considerations, and security considerations.
    - The conference expects that many papers will be foundational research and not tied to particular applications, let alone deployments. However, if there is a direct path to any negative applications, the authors should point it out. For example, it is legitimate to point out that an improvement in the quality of generative models could be used to generate deepfakes for disinformation. On the other hand, it is not needed to point out that a generic algorithm for optimizing neural networks could enable people to train models that generate Deepfakes faster.
    - The authors should consider possible harms that could arise when the technology is being used as intended and functioning correctly, harms that could arise when the technology is being used as intended but gives incorrect results, and harms following from (intentional or unintentional) misuse of the technology.
    - If there are negative societal impacts, the authors could also discuss possible mitigation strategies (e.g., gated release of models, providing defenses in addition to attacks, mechanisms for monitoring misuse, mechanisms to monitor how a system learns from feedback over time, improving the efficiency and accessibility of ML).

11. **Safeguards**

    Question: Does the paper describe safeguards that have been put in place for responsible release of data or models that have a high risk for misuse (e.g., pretrained language models, image generators, or scraped datasets)?

Answer: [NA]

Justification: Our paper studies a specific bottleneck in a purely synthetic context that is of broad interest to the BED community but which we believe does not raise any significant safety issues.

Guidelines:

- The answer NA means that the paper poses no such risks.
- Released models that have a high risk for misuse or dual-use should be released with necessary safeguards to allow for controlled use of the model, for example by requiring that users adhere to usage guidelines or restrictions to access the model or implementing safety filters.
- Datasets that have been scraped from the Internet could pose safety risks. The authors should describe how they avoided releasing unsafe images.
- We recognize that providing effective safeguards is challenging, and many papers do not require this, but we encourage authors to take this into account and make a best faith effort.

12. **Licenses for existing assets**

    Question: Are the creators or original owners of assets (e.g., code, data, models), used in the paper, properly credited and are the license and terms of use explicitly mentioned and properly respected?

    Answer: [Yes]

    Justification: We have credited all models, enviornments and libraries that we used in our experiments.

    Guidelines:

    - The answer NA means that the paper does not use existing assets.
    - The authors should cite the original paper that produced the code package or dataset.
    - The authors should state which version of the asset is used and, if possible, include a URL.
    - The name of the license (e.g., CC-BY 4.0) should be included for each asset.
    - For scraped data from a particular source (e.g., website), the copyright and terms of service of that source should be provided.
    - If assets are released, the license, copyright information, and terms of use in the package should be provided. For popular datasets, `paperswithcode.com/datasets` has curated licenses for some datasets. Their licensing guide can help determine the license of a dataset.
    - For existing datasets that are re-packaged, both the original license and the license of the derived asset (if it has changed) should be provided.
    - If this information is not available online, the authors are encouraged to reach out to the asset's creators.

13. **New assets**

    Question: Are new assets introduced in the paper well documented and is the documentation provided alongside the assets?

    Answer: [NA]

    Justification: We have not provided any new assets in this paper.

    Guidelines:

    - The answer NA means that the paper does not release new assets.
    - Researchers should communicate the details of the dataset/code/model as part of their submissions via structured templates. This includes details about training, license, limitations, etc.
    - The paper should discuss whether and how consent was obtained from people whose asset is used.
    - At submission time, remember to anonymize your assets (if applicable). You can either create an anonymized URL or include an anonymized zip file.

14. **Crowdsourcing and research with human subjects**

    Question: For crowdsourcing experiments and research with human subjects, does the paper include the full text of instructions given to participants and screenshots, if applicable, as well as details about compensation (if any)?

    Answer: [NA]

    Justification: We have not used any crowdsurcing or human subjects in this research.

    Guidelines:

    - The answer NA means that the paper does not involve crowdsourcing nor research with human subjects.
    - Including this information in the supplemental material is fine, but if the main contribution of the paper involves human subjects, then as much detail as possible should be included in the main paper.
    - According to the NeurIPS Code of Ethics, workers involved in data collection, curation, or other labor should be paid at least the minimum wage in the country of the data collector.

15. **Institutional review board (IRB) approvals or equivalent for research with human subjects**

    Question: Does the paper describe potential risks incurred by study participants, whether such risks were disclosed to the subjects, and whether Institutional Review Board (IRB) approvals (or an equivalent approval/review based on the requirements of your country or institution) were obtained?

    Answer: [NA]

    Justification: We have not used any crowdsurcing or human subjects in this research.

    Guidelines:

    - The answer NA means that the paper does not involve crowdsourcing nor research with human subjects.
    - Depending on the country in which research is conducted, IRB approval (or equivalent) may be required for any human subjects research. If you obtained IRB approval, you should clearly state this in the paper.
    - We recognize that the procedures for this may vary significantly between institutions and locations, and we expect authors to adhere to the NeurIPS Code of Ethics and the guidelines for their institution.
    - For initial submissions, do not include any information that would break anonymity (if applicable), such as the institution conducting the review.

16. **Declaration of LLM usage**

    Question: Does the paper describe the usage of LLMs if it is an important, original, or non-standard component of the core methods in this research? Note that if the LLM is used only for writing, editing, or formatting purposes and does not impact the core methodology, scientific rigorousness, or originality of the research, declaration is not required.

    Answer: [No]

    Justification: This research does not concern LLMs.

    Guidelines:

    - The answer NA means that the core method development in this research does not involve LLMs as any important, original, or non-standard components.
    - Please refer to our LLM policy (`https://neurips.cc/Conferences/2025/LLM`) for what should or should not be described.